Establishment of urban waterlogging pre-warning system based on coupling RBF-NARX neural networks

Ming Wei, Lin She and Xue-yi You

ABSTRACT

The optimal layout of low-impact development (LID) facilities satisfying annual runoff control for low rainfall expectation is not effective under extreme rainfall conditions and urban waterlogging may occur. In order to avoid the losses of urban waterlogging, it is particularly significant to establish a waterlogging early warning system. In this study, based on coupling RBF-NARX neural networks, we establish an early warning system that can predict the whole rainfall process according to the rainfall curve of the first 20 minutes. Using the predicted rainfall process curve as rainfall input to the rainfall-runoff calculation engine, the area at risk of waterlogging can be located. The results indicate that the coupled neural networks perform well in the prediction of the hypothetical verification rainfall process. Under the studied extreme rainfall conditions, the location of 25 flooding areas and flooding duration are well predicted by the early warning system. The maximum of average flooding depth and flooding duration is 16.5 cm and 99 minutes, respectively. By predicting the risk area and the corresponding flooding time, the early warning system is quite effective in avoiding and reducing the losses from waterlogging.

Key words | NARX neural network, pre-warning system, RBF neural network, urban waterlogging

HIGHLIGHTS

- A pre-warning urban waterlogging system is established and applied.
- The whole rainfall process is predicted by the first 20 minutes rainfall using the combined RBF and NARX neural networks.
- The waterlogging risk area and overflow time are well predicted.

Ming Wei
Lin She
Xue-yi You (corresponding author)
Tianjin Engineering Center of Urban River Eco-purification Technology, School of Environmental Science and Engineering,
Tianjin University,
Tianjin 300350,
China
E-mail: *xyyou@tju.edu.cn*

doi: 10.2166/wst.2020.477

GRAPHICAL ABSTRACT

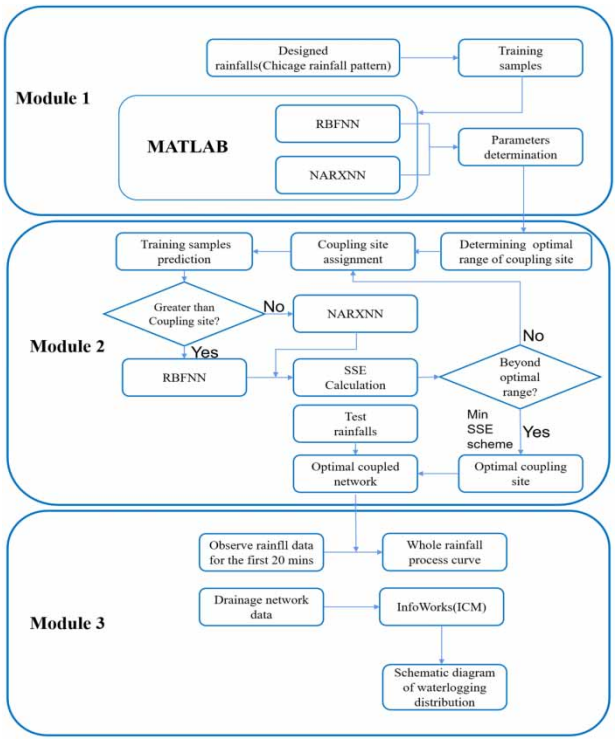

INTRODUCTION

The rapid urbanization process, especially in China, has caused the original green areas to be continuously replaced by gray buildings, and thus the impervious surface has increased on a large scale. In addition, the occurrence of extreme weather is increasingly frequent around the world (Zhou 2014; Paule-Mercado *et al.* 2017).

Recently, China has developed a new concept of the sponge city based on the 'low-impact development' (LID) concept proposed by the USA in the 1990s, which provides a natural and low-impact development approach for urban stormwater management (Ahiablame *et al.* 2012; Kong *et al.* 2017). A series of policies were then promulgated by China, including the 'Sponge City Construction Technology Guide (Trial)' (Technical Guide 2015). According to these policies, the annual runoff control rate was used as the control target for the total runoff control of low-impact development. In the optimization research for this study, the annual runoff control rate was also selected as the control target.

Urban waterlogging mainly occurs when short-term heavy rainstorms' precipitation exceeds the drainage capacity of a city (Yin *et al.* 2011; Hammond *et al.* 2015; Xue *et al.* 2016). Under such circumstance, the establishment of an urban waterlogging early warning system is particularly important. In order to realize the construction of early warning systems, researchers have proposed several systems (Chen *et al.* 2015; Wang *et al.* 2019; Wei *et al.* 2019). By dividing an urban area into many spatial grid cells, the model could simulate surface runoff routing and determine the inundation index (Chen *et al.* 2015). Capturing the rapid generation of surface runoff in urban areas during heavy rainfall, the directions of horizontal inflow and outflow were determined dynamically during each time step (Wang *et al.* 2019). Based on WEBGIS technology, a visual waterlogging monitoring and early warning platform was developed. The functions of multi-source rainfall monitoring in urban areas and real-time display of forecasted waterlogging were realized (Wei *et al.* 2019). However, the above-mentioned research focused only on the simulation of surface runoff without involving the prediction of extreme rainfall events causing waterlogging.

In the design of flood warning systems, rainfall forecasting is deemed to be quite significant (Nasseri *et al.* 2008). As a prediction model, the neural network is a preferable choice since it can map any nonlinear function without requiring to understand the laws of physics. (Jain & Kumar 2007; Nasseri *et al.* 2008). By coupling neural networks (like RBF-NN) with a genetic algorithm, high forecasting accuracy of rainfall process was obtained (Nasseri *et al.* 2008; Wu *et al.* 2015). She & You (2019) coupled Radical Basis Function (RBF) and Nonlinear Auto-Regressive models with Exogenous Inputs (NARX) to build a model for the prediction of urban drainage outflow curves. Results indicated that the Square Sum of Error (SSE) between network prediction and SWMM simulation was only 0.273.

In this research, the coupled artificial networks of RBF and NARX and the drainage model were used to establish an effective waterlogging early warning system. The early warning system can predict the whole rainfall process based on the first 20 minutes of rainfall and then it starts to calculate the drainage model to realize the distribution prediction of urban waterlogging areas in the study area. The prediction results of early warning system can be notified to drivers and pedestrians in the form of electronic street signs and FM broadcasts to avoid coming into the areas with serious urban waterlogging, and further reduce the loss of vehicle property and personal safety.

METHODOLOGY

Study area

The study area is located in Tianjin at the northern part of north China Plain. It is one of the demonstration areas of the National Sponge City Construction Project. The average annual rainfall is 360–970 mm, and the annual precipitation is mainly concentrated in summer. The terrain in the study area is relatively flat, and the overall terrain gradually increases from northwest to southeast. The terrain elevation in most areas of the region is between 1.86 and 3.9 meters, and the maximum elevation is 13.038 meters. Moreover, the area is divided into seven independent rainwater systems, and the rainwater systems in the adjacent areas NO.1 and NO.2 are selected as the research object in this paper.

Figure 1 shows the interpretation results of the underlying surface in the study area, apparently, the study area is highly urbanized with few 'sponge' elements. The area NO.1 is 1.812 square kilometers, of which more than 38% are impervious pavement and building roofs, while green land only accounts for 16%, and the rest is composed of sidewalks, urban bare land and parking lots. Area NO.2 is 2.46 square kilometers, of which impermeable pavement and building roofs account for 5.22 and 30%, respectively, and urban green land only accounts for 16.57%.

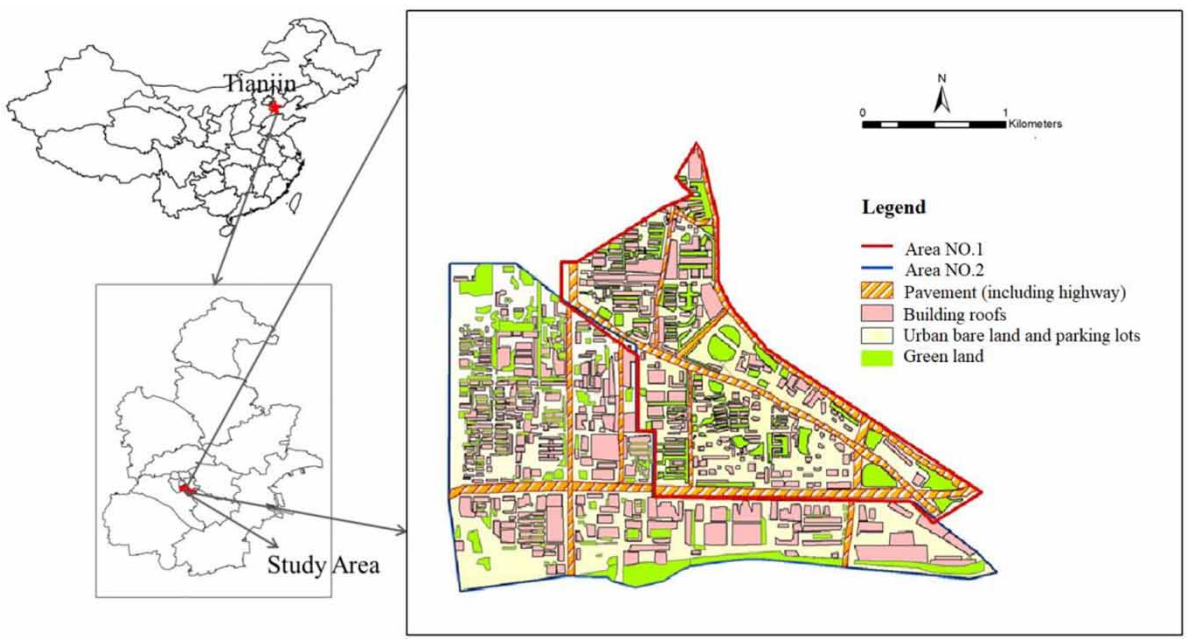

Figure 1 | Schematic diagram of the location and the type of land used of the study area.

The necessity of system establishment

The InfoWorks (ICM) software was used to simulate the situation of waterlogging of the urban drainage system under extreme rainfall conditions and the Theissen polygon rule was used as the criteria for dividing the catchment into sub-catchments. Under the extreme rainfall conditions of recurrence period 10 years and duration 1 h, the node overflow and pipeline load of the optimal LID layout area of NO.1 and NO.2 are shown in Figures 2 and 3. It is clearly seen from Figures 2 and 3 that despite the sponge facilities in the study area, all pipelines are overloaded, and several nodes are overflowed. And the maximum overflow volume is 1,205.5 m^3 under an extreme rainfall condition. Obviously, under such extreme rainfall conditions, the optimal layout of LID with annual runoff control of low return period as the optimization goal is not ideal way for the runoff control of extreme rainfall.

In general, when the volume of overflowed runoff is too large, a mass of rainwater accumulated on the road surface will cause serious harm to urban traffic and pedestrian safety. With the pre-warning system, the flooding areas will be notified to pedestrians and drivers via electronic street signs and FM broadcasts before the formation of a waterlogging area, so it can reduce the losses caused by waterlogging. The waterlogging pre-warning system is of great importance.

Selection of neural network

There are many types of artificial neural networks with different functions, and researchers select the neural

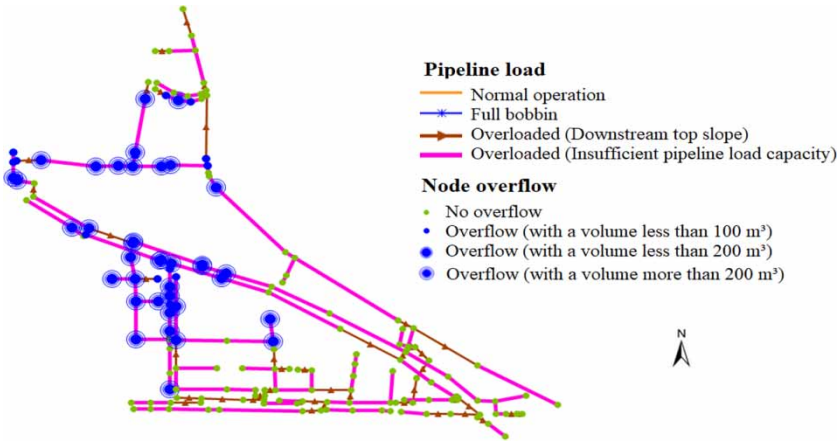

Figure 2 | Node overflow and pipeline load in the optimal LID layout area NO.1.

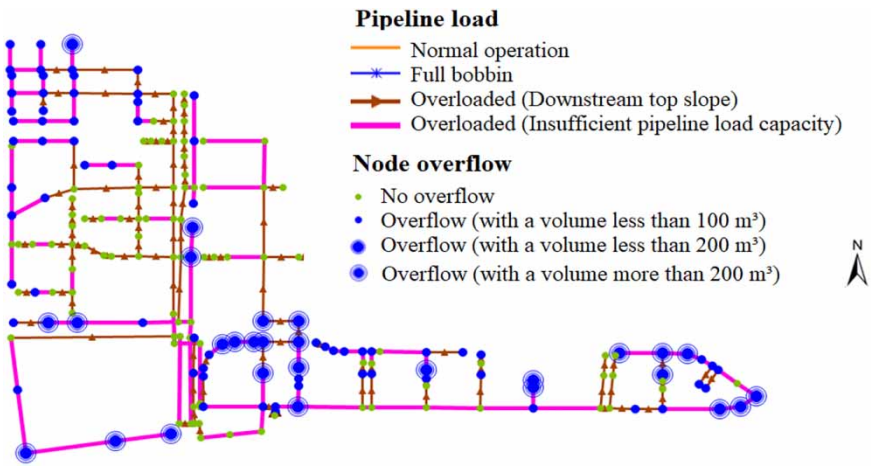

Figure 3 | Node overflow and pipeline load of optimal layout in area NO.2.

network with corresponding functions in accordance with the application requirements in practical problems. According to whether they have feedback and memory functions, neural networks are divided into static neural networks and dynamic neural networks. From the research and application of static neural networks and dynamic neural networks (Wang *et al.* 2010; Wu *et al.* 2015; Chang *et al.* 2016; Lee *et al.* 2016; Safari *et al.* 2016; Supratid *et al.* 2017; Marcjasz *et al.* 2018), it was found that static neural networks (for example the RBF network) have good performance of prediction on non-monotonic intervals, while dynamic neural networks (for example the NARX network) shows high-precision prediction in monotone intervals (She & You 2019). Therefore, in the prediction of the rainfall process, the advantages of the RBF neural network (RBF-NN) and the NARX neural network (NARX-NN) were coupled to establish a coupling RBF-NARX neural network to predict the extreme rainfall process by the initial 20 minutes rainfall.

Data preparation and network parameter optimization

The Chicago rain pattern is widely used as a design rainfall pattern based on the intensity-duration-frequency relationship, which is suitable for the time allocation of urban short-duration intensive design rainfall. The design rainfall considered was a single-peak rainfall and the formula of Chicago rainfall pattern in the local area was:

$$q = \frac{2141 \times (1 + 0.7562 \lg P)}{(T + 9.6093)^{0.6893}} \tag{1}$$

where, q stands for the intensity of design rainfall $[L/(s \cdot hm^2)]$; P stands for rainfall return period (years); T is the duration of the design rainfall (min).

In this study, nine sets of design rainfall were used as the data set for training the coupled network. The output of the RBF neural network was expressed as (Huang *et al.* 2005):

$$yj = \sum_{i=1}^{h} wij \exp\left(-\frac{1}{2\sigma^2}\|xp - ci\|^2\right) \tag{2}$$

where, x_p is the input sample, $(p = 1,2,3\ldots,P)$, and P is the total number of samples; c_i is the Gaussian function center of each hidden layer node; y_j is the actual output of the j-th output node of the network corresponding to the input sample $(j = 1, 2, 3, \ldots n)$, and n is the number of output nodes; w_{ij} is the connection weight of the hidden layer to the output layer, σ is the variance of the Gaussian function; h is the number of hidden layer nodes.

The expression of the NARX network output is (Siegelmann *et al.* 1997):

$$y(t) = f(y(t-1), y(t-2), \cdots, y(t-n_y), x(t), x(t-1), \cdots, x(t-n_x)) \tag{3}$$

where, $x(t)$ and $y(t)$ are the input and output of the network, respectively; nx and ny are the delay orders of the input and output of the network, respectively.

The designed rainfall curves were discretized by minute and the rainfall intensity of the initial 20 minutes was applied as the input data of the neural networks, while the rainfall intensity of the whole rainfall process was used as the ideal output of the neural networks for checking the accuracy of the prediction of the neural networks. The randomly selected design rainfalls for training and validating neural networks are shown in Table 1. Since the rainfall curves were discretized by minute, the data number of each set of design rainfall corresponded to the duration of the rainfall.

RBF-NN and NARX-NN were set up separately. Among the nine sets of design rainfall, one set was chosen randomly as the validation set and the rest were used as the training sets. A set of test data was generated separately using the local area Chicago rainfall pattern formula. The recurrence period, duration and peak coefficient of test data were 25.8 years, 212 minutes and 0.14, respectively.

Table 1 | Rainfall data sets for training and validating neural networks

Rainfall recurrence period (year)	Duration of rainfall (min)	Rain capacity (mm)	Rain peak coefficient
3.4	91	68.65	0.22
4.1	109	76.48	0.41
7.6	131	93.06	0.76
9.5	87	83.67	0.55
13.3	71	82.41	0.34
16.6	177	119.18	0.61
17.7	113	102.91	0.48
18.7	99	99.03	0.69
19.5	124	108.19	0.72

In order to attain the best prediction accuracy from the neural network, the optimal number of hidden neurons and the spread needed to be determined for RBF-NN. While in the NARX network, except for the number for hidden neurons, the optimal network input and output delay orders should also be determined.

During the training process of the network, the RBF and NARX were trained respectively to determine the optimal network parameter until the minimum MSE was obtained, otherwise they returned back to begin a new training process. This program loop could optimize the network parameters within a certain range of values, and the training errors of the network were calculated under different parameters respectively. Under the premise that the network was not over-trained, the number of hidden neurons, the spread, and the network input and output delay ordered with the smallest error were served as network parameters. The optimized results of the parameters are listed in Table 2. The detailed parameter optimization principle and process referred to the reference of She & You (2019).

Network coupling and training

The above trained networks were applied to predict the rainfall process curves according to the prediction interval of the NARX-NN and RBF-NN discussed in She & You (2019). According to the superior prediction interval of the NARX network and RBF network discussed in the Data preparation and network parameter optimization section, the rainfall process curve to be predicted was divided into a monotonic interval and a non-monotonic interval. For the non-monotonic interval above the coupling site, the RBF network was used to predict the rainfall process, and for the monotonic interval below the coupling site, the NARX network was used to predict the rainfall process.

To fully reflect the global error of network prediction under different coupling sites, the Square Sum of Error (SSE) were used to calculate the error of prediction. The SSE of the network prediction at different coupling sites during the training process is illustrated in Figure 4. The prediction error of the network was mainly from the place near the peak of rain intensity. When the coupling site was taken as 130 mm/h, the SSE predicted by the network was at a minimum. It was found that the point of rainfall intensity of 130 mm/h should be selected as the coupling site for the RBF-NN and NARX-NN in the present study.

Table 2 | Optimization value of neural network parameters

Type of neural network	Parameters	Optimization value
RBF-NN	Number of hidden layer nodes	24
	Spread	0.8
NARX-NN	Number of hidden layer nodes	8
	Input and output delay orders	1:8, 1:8

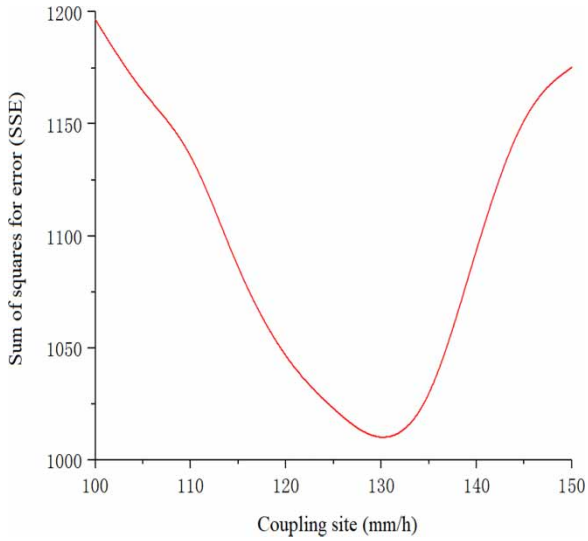

Figure 4 | Accumulation and variance at different rainfall intensities.

The training and testing process curves of the coupled network are shown in Figure 5. The predicted mean square error (MSE) is shown as follows:

$$MSE = \frac{1}{N}\sum_{n=1}^{N}(yn - \hat{y}n)^2 \quad (4)$$

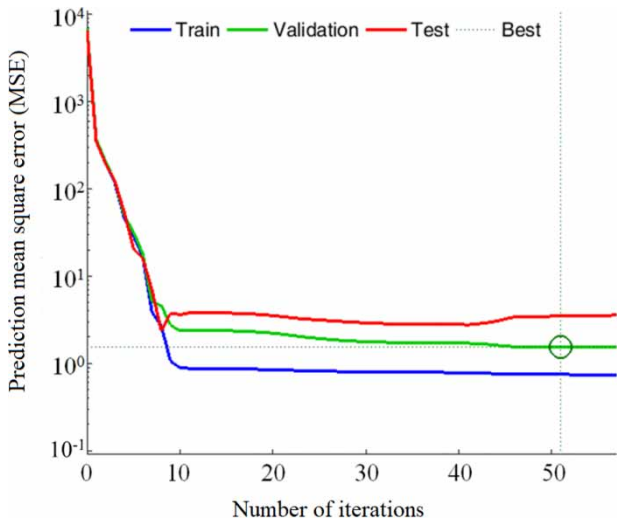

Figure 5 | Training results of coupling neural network.

where, N stands for the total number of data sets; yn is the true value; and $\hat{y}n$ is the predicted value of rainfall.

As the number of iterations increases, the predicted MSE of the rainfall data of training, verification, and testing decreased gradually. At the 51th iteration step, the minimum verification process curve was obtained.

The results of training indicated that there was no overfitting phenomenon when the coupled network was fully trained. Therefore, the trained coupled network could be employed to predict the whole rainfall process curve.

Prediction of whole rainfall intensity by initial 20 min rainfall

The rain process curves of the generated rainfall were discretized by minute and the rainfall intensity of the initial 20 minutes was applied as the input data of the neural network. Then the data of the whole rainfall intensity of the entire rainfall process could be predicted by the coupled neural networks and the predicted rainfall was adopted as the actual rainfall in the waterlogging pre-warning system.

RESULTS OF PRE-WARNING SYSTEM

In this study, the random number method was adopted to generate a simulated actual rainfall to test the validity of the coupled neural networks. The recurrence period, duration and peak coefficient of the simulated actual rainfall were chosen randomly as 5.7 years, 117 minutes and 0.37, respectively, and its initial 20 minutes rainfall intensity was used to replace the initial 20 minutes rainfall intensity actually measured by the rainfall sensor located in the prediction area for the waterlogging pre-warning system. Then the initial 20 minutes rainfall intensity was input into the trained coupled neural networks to predict the rainfall intensity of the whole rainfall, and the results are shown in Figure 6.

When the rainfall intensity is small, the feedback and memory functions of the NARX network fit the rainfall process curve well to make a coupled network with high prediction accuracy. Due to the large variation of rain intensity near the rain peak and the weak mapping relationship between the peak rainfall and the initial rainfall, the prediction error of the coupled network is large and the peak prediction relative error is 3.44%. The calculation results showed that the prediction mean square error (MSE) of the coupled neural networks is 2.51, which indicated that the coupled neural networks could accurately predict the

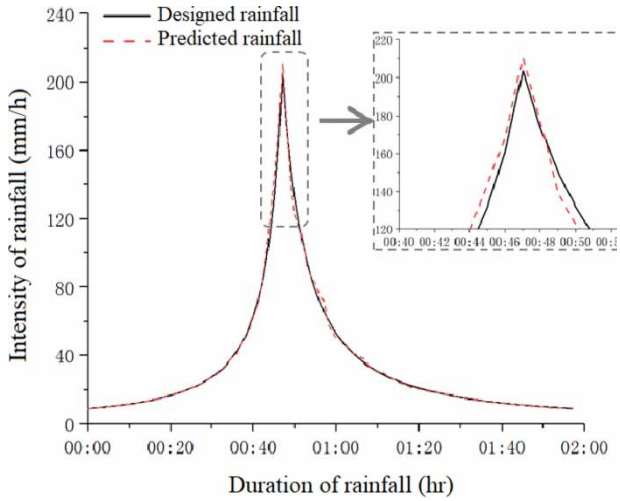

Figure 6 | Prediction of simulated actual rainfall by coupled neural networks.

extreme rainfall and the prediction rainfall could be used in the calculation of waterlogging pre-warning system.

Based on the prediction of the extreme rainfall process, the pre-warning system calls the rainfall-runoff engine to calculate the waterlogging situation in the study area under the optimal layout of low impact development. In this study, the average waterlogging depth was used to evaluate the waterlogging disasters in each sub-catchment (Wang *et al.* 2017), which could be calculated as follows:

$$h_j = \sqrt{\frac{i_j V_j}{W_j}} \tag{5}$$

where, h_j stands for the average waterlogging depth of sub-catchment j (cm); V_j is the overflow volume of the node in sub-catchment j (m^3); Wj and i_j are the width (m) and slope (%) of sub-catchment j, respectively.

In the study, the case where the average waterlogging depth was less than 1 cm was regarded as no urban waterlogging, and where the average waterlogging depth was between 1 to 5 cm, 5 to 10 cm and greater than 10 cm was defined as mild, moderate and severe waterlogging, respectively. The distribution of average waterlogging depth of each sub-catchment during the simulation period is shown in Figures 7 and 8, and the waterlogging period is listed in Table 3.

In area NO.1, there are multiple sub-catchments of waterlogging disaster that occur, including 21 sub-catchment areas with mild waterlogging, and one sub-catchment area with moderate and severe waterlogging each, separately. The sub-catchment area with severe waterlogging is Y-123,

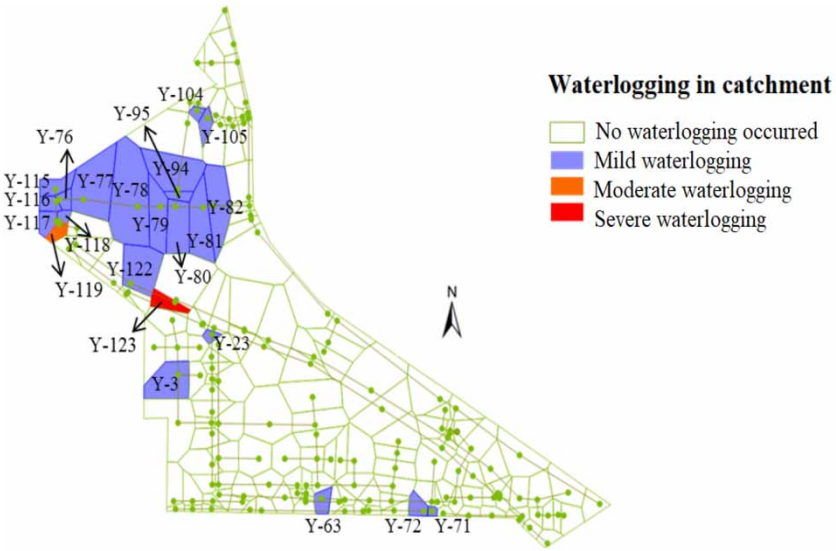

Figure 7 | Waterlogging distribution in area NO.1.

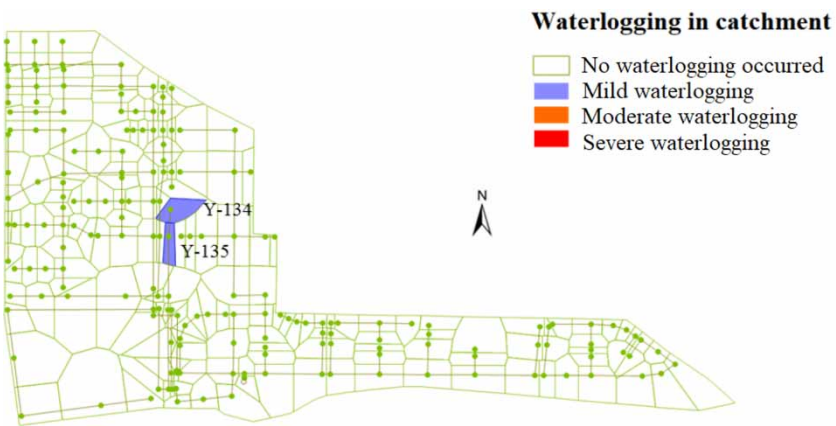

Figure 8 | Waterlogging distribution in area NO.2.

where the average waterlogging depth is 16.5 cm. In terms of waterlogging period, there are seven sub-catchments with a waterlogging duration of more than 1 hour. Y-116 is the sub-catchment with the earliest occurrence of waterlogging. It begins to flood at the 21st minute of rainfall, and the waterlogging duration is 99 minutes. It is also the sub-catchment area with the longest flood period in the area NO.1.

From Table 3 and Figure 8, it was obvious that the urban waterlogging was less serious in area NO.2. Only moderate waterlogging occurs in the Y-134 and Y-135 sub-catchments, with an average waterlogging depth of 2.4 cm and 1.2 cm, respectively. As for the period of waterlogging, the Y-134 and Y-135 sub-catchments begin to flood at the 23rd and 27th minutes of rainfall, respectively, and the corresponding duration of waterlogging is 92 and 27 minutes, separately. Compared with area NO.1, the extreme rainfall has a smaller impact on area NO.2, and the LID facility stagnates a large amount of rainwater in an initial period of rainfall. Comparing with Figure 1, it was concluded that the occurrence of waterlogging in sub-catchments is closely related to the type of land use. Mild waterlogging always occurred in sub-catchments with dense buildings and little green land. In Area 1, the main type of land use in sub-catchments with moderate waterlogging are pavements, urban bare land and parking lots, and the main land types in sub-catchments with severe waterlogging are pavements.

Based on the prediction of the average waterlogging depth and waterlogging period, the urban waterlogging

Table 3 | The waterlogging period in catchments of the study area

Area	Number of sub-catchment	Beginning time	Ending time	Duration of waterlogging (min)
NO.1	Y-104	0:22	1:26	64
	Y-105	0:26	1:18	52
	Y-115	0:22	1:56	94
	Y-116	0:21	2:00	99
	Y-117	0:32	1:41	69
	Y-118	0:34	1:36	62
	Y-119	0:32	1:36	64
	Y-122	0:43	1:12	29
	Y-123	0:33	1:30	57
	Y-28	0:47	0:49	2
	Y-3	0:48	0:57	9
	Y-63	0:24	0:43	19
	Y-71	0:23	0:42	19
	Y-72	0:22	0:46	24
	Y-76	0:33	1:32	59
	Y-77	0:35	1:27	52
	Y-78	0:32	1:34	62
	Y-79	0:33	1:30	57
	Y-80	0:38	1:15	37
	Y-81	0:44	1:08	24
	Y-82	0:46	1:03	17
	Y-94	0:32	1:19	47
	Y-95	0:31	1:25	54
NO.2	Y-134	0:23	1:55	92
	Y-135	0:27	0:54	27

early warning system predicts real-time information on waterlogging distribution, water depth and ponding time from the beginning to end of the forecast area and transmits the forecast information to the media platform, where the electronic road signs, mobile phone alarming, short message and FM broadcasting notify the drivers and pedestrians to avoid areas of moderate and severe waterlogging to ensure the safety of citizens' property and daily travel.

DISCUSSION

To order the making of a city with a high ability to cope with extreme rainfall events and avoid the waterlogging that seriously threatens urban safety and socioeconomic development, the establishment of a rainfall pre-warning system is urgent and necessary. By coupling static and dynamic neural networks, and combining the coupled neural networks with a drainage model, a waterlogging early warning system was established and applied in one of the demonstration areas of the Sponge City Construction Project in Tianjin. The system was expected to realize the prediction of the entire process of rainfall based on the initial 20 minutes rainfall trend, and it achieved the forecasting of the waterlogging distribution in catchments by calling the drainage model. Thus, the research laid a preliminary application for the construction of future smart cities and urban intelligent drainage systems.

In the studies conducted by Chen *et al.* (2015), Wang *et al.* (2019) and Wei *et al.* (2019), the precipitation data were from the corresponding centers for environmental information (Wang *et al.* 2019; Wei *et al.* 2019), digital weather radar-based precipitation estimation and rain gauge observed precipitation (Chen *et al.* 2015). Unlike the above methods, the proposed model in this paper developed the rainfall process curves based on the rainfall trend of the initial 20 minutes is better to predicate the urban flood management without the need of the other department cooperation. Since the fore-mentioned warning systems built by scholars are based on digital weather radar and field observations, their warning systems are very different from ours that using artificial neural network to predict the rainfall and inforworks to find the waterlogging distribution. Therefore, it was hard to compare our early warning system with theirs.

Nevertheless, the intelligent application in the construction of sponge cities is still in the theoretical assumption stage although the corresponding intelligent control technologies are applied to specific low-impact development facilities. In this study, the predicted extreme rainfall by the initial 20 minutes rainfall was realized. However, the predicated rain was a Chicago rainstorm, which was still too ideal for actual rainfall. The subsequent research should be studied with actual rainfall to verify the effectiveness of the proposed predication method. The further study on the application of intelligent technology in smart water affairs is very necessary.

CONCLUSION

The establishment of an urban early warning system for waterlogging based on current norms and simulation results for extreme rainfall was discussed. After completing the data preparation, the authors selected the coupled neural network of the RBF and NARX networks as the prediction tool for the actual rainfall of the waterlogging early warning system. The optimization the parameters and coupling sites of relevant networks was completed in the process of network training. Using the trained coupled network, the system could accurately predict the rainfall process of extreme rainfall, and the mean square error (MSE) of the

network prediction was only 2.51. Based on the prediction of the extreme rainfall process, the rainfall-runoff engine for calculation was called, and could obtain the waterlogging situation of each sub-catchment in the study area. According to the statistics, waterlogging occurs in 23 sub-catchments of NO.1 area, where the maximum average waterlogging depth is 16.5 cm and the maximum waterlogging duration is 99 minutes. Nevertheless, only two sub-catchments in area NO.2 flooded. The largest average waterlogging depth is 2.4 cm, and the maximum waterlogging duration is 92 minutes. The above approach established a good urban early warning system for waterlogging distribution, which could be used in the near future.

ACKNOWLEDGEMENTS

This work was supported by the Tianjin technical innovation guidance project program (16YDLJSF00030) and the key projects in the control and management of national polluted water bodies (2017ZX07106001).

DATA AVAILABILITY STATEMENT

All relevant data are included in the paper or its Supplementary Information.

REFERENCES

Ahiablame, L. M., Engel, B. A. & Chaubey, I. 2012 Effectiveness of low impact development practices: literature review and suggestions for future research. *Water, Air, Soil Pollut* **223** (7), 4253–4273.

Chang, F. J., Chang, L. C., Huang, C. W. & Kao, I. F. 2016 Prediction of monthly regional groundwater levels through hybrid soft-computing techniques. *Journal of Hydrology* **541**, 965–976.

Chen, Y. B., Zhou, H. L., Zhang, H., Du, G. M. & Zhou, J. H. 2015 Urban flood risk warning under rapid urbanization. *Environmental Research* **139**, 3–10.

Hammond, M. J., Chen, A. S., Djordjevic, S., Butler, D. & Mark, O. 2015 Urban flood impact assessment: a state-of-the-art review. *Urban Water Journal* **12** (1), 14–29.

Huang, G. B., Saratchandran, P. & Sundararajan, N. 2005 A generalized growing and pruning RBF (GGAP-RBF) neural network for function approximation. *IEEE Transactions on Neural Networks* **16** (1), 57–67.

Jain, A. & Kumar, A. M. 2007 Hybrid neural network models for hydrologic time series forecasting. *Applied Soft Computing* **7**, 585–592.

Kong, F., Ban, Y., Yin, H., James, P. & Dronova, I. 2017 Modeling stormwater management at the city district level in response to changes in land use and low impact development. *Environmental Modelling and Software* **95**, 132–142.

Lee, C. C., Sheridan, S. C., Barnes, B. B., Hu, C. M., Pirhalla, D. E., Ransibrahmanakul, V. & Shein, K. 2016 The development of a non-linear autoregressive model with exogenous input (NARX) to model climate-water clarity relationships: reconstructing a historical water clarity index for the coastal waters of the southeastern USA. *Theoretical & Applied Climatology* **130**, 557–569.

Marcjasz, G., Uniejewski, B. & Weron, R. 2018 On the importance of the long-term seasonal component in day-ahead electricity price forecasting with NARX neural networks. *International Journal of Forecasting* **35** (4), 1520–1532.

Nasseri, M., Asghari, K. & Abedini, M. J. 2008 Optimized scenario for rainfall forecasting using genetic algorithm coupled with artificial neural network. *Expert Systems with Applications* **35**, 1415–1421.

Paule-Mercado, M. A., Lee, B. Y., Memon, S. A., Umer, S. R. & Salim, I. 2017 Influence of land development on stormwater runoff from a mixed land use and land cover catchment. *Science of the Total Environment* **599**, 2142–2155.

Safari, M. J. S., Aksoy, H. & Mohammadi, M. 2016 Artificial neural network and regression models for flow velocity at sediment incipient deposition. *Journal of Hydrology* **541**, 1420–1429.

She, L. & You, X. Y. 2019 A dynamic flow forecast model for urban drainage using the coupled artificial neural network. *Water Resources Management* **33** (9), 3143–3153.

Siegelmann, H. T., Horne, B. G. & Giles, C. L. 1997 Computational capabilities of recurrent NARX neural networks. *IEEE Transactions on Systems, Man, and Cybernetics, Part B (Cybernetics)* **27** (2), 208–215.

Supratid, S., Aribarg, T. & Supharatid, S. 2017 An integration of stationary wavelet transform and nonlinear autoregressive neural network with exogenous input for baseline and future forecasting of reservoir inflow. *Water Resources Management* **31**, 4023–4043.

Technical Guide for Construction of Sponge City of Rainwater System for Low Impact Development (Trial) 2015 China Construction Industry Press (in Chinese).

Wang, M., Sun, Y. & Sweetapple, C. 2017 Optimization of storage tank locations in an urban stormwater drainage system using a two-stage approach. *Journal of Environmental Management* **204**, 31–38.

Wang, W., Li, X., Wang, C. & Zhao, H. C. 2010 River water level forecast based on spatio-temporal series model and RBF neural network. In: *International Conference on Information Science & Engineering*. IEEE.

Wang, X. Q., Kinsland, G., Poudel, D. & Fenech, A. 2019 Urban flood prediction under heavy precipitation. *Journal of Hydrology* **577**, 123984.

Wei, J., Yu, H. Y., Hu, H. F., Peng, X. Y. & Chen, X. L. 2019 Development and application of urban waterlogging meteorological risk monitoring and early warning system in Shijiazhuang. *China Rural Water and Hydropower* (2), 34–38&43 (in Chinese).

Wu, J. S., Long, J. & Liu, M. Z. 2015 Evolving RBF neural networks for rainfall prediction using hybrid particle swarm optimization and genetic algorithm. *Neurocomputing* **148**, 136–142.

Xue, F., Huang, M., Wang, W. & Zou, L. 2016 Numerical simulation of urban waterlogging based on flood area model. *Advances in Meteorology* **1**, 1–9.

Yin, Z., Yin, J., Xu, S. & Wen, J. 2011 Community-based scenario modelling and disaster risk assessment of urban rainstorm waterlogging. *Journal of Geographical Sciences* **21** (2), 274–284.

Zhou, Q. 2014 A review of sustainable urban drainage systems considering the climate change and urbanization impacts. *Water* **6** (4), 976–992.

First received 9 July 2020; accepted in revised form 23 September 2020. Available online 6 October 2020